

A THERMODYNAMIC DESCRIPTION OF METASTABLE c-TiAlZrN COATINGS WITH TRIPLE SPINODALLY DECOMPOSED DOMAINS

J. Zhou ^{a,b}, L. Zhang ^{a,*,#}, L. Chen ^a, Y. Du ^a, Z.-K. Liu ^c

^a Central South University, State Key Laboratory of Powder Metallurgy, Changsha, Hunan, China

^b Lanzhou Institute of Technology, Department of Material Engineering, Lanzhou, Gansu, China

^c Pennsylvania State University, Department of Materials Science and Engineering, University Park, USA

(Received 17 October 2016; accepted 27 December 2016)

Abstract

A critical thermodynamic assessment of the metastable c-TiAlZrN coatings, which are reported to spinodally decompose into triple domains, i.e., c-TiN, c-AlN, and c-ZrN, was performed via the CALculation of PHase Diagram (CALPHAD) technique based on the limited experimental data as well as the first-principles computed free energies. The metastable c-TiAlZrN coatings were modeled as a pseudo-ternary phase consisting of c-TiN, c-AlN and c-ZrN species, and described using the substitutional solution model. The thermodynamic descriptions for the three boundary binaries were directly taken from either the CALPHAD assessment or the first-principles results available in the literature except for a re-adjustment of the pseudo-binary c-AlN/c-ZrN system based on the experimental phase equilibria in the pseudo-ternary system. The good agreement between the calculated phase equilibria and the experimental data over the wide temperature range was obtained, validating the reliability of the presently obtained thermodynamic descriptions for the c-TiAlZrN system. Based on the present thermodynamic description, different phase diagrams and thermodynamic properties can be easily predicted. It is anticipated that the present thermodynamic description of the metastable c-TiAlZrN coatings can serve as the important input for the later quantitative description of the microstructure evolution in c-TiAlZrN coatings during service life.

Keywords: c-TiAlZrN coatings; Metastable phase; Spinodal decomposition; CALPHAD

1. Introduction

Aluminium based ternary transition metal nitrides with cubic NaCl (c) structure have been utilized as hard and protective coatings for advanced machining and other high temperature service environments due to their high hardness, thermal stability, and oxidation resistance [1-4]. Among them, the metastable c-Ti_{1-x}Al_xN coatings with x < 0.7 deposited via physical vapor deposition (PVD) are the most widely used coatings due to their superior wear resistance resulting from the formation of stable oxide layers on the surface of the coatings. Good oxidation resistance and high thermal stability of the hard coatings are the key properties for many industrial applications. c-TiAlN coatings were found oxidizing at 850 °C [5] and then forming a dense Al₂O₃ scales, which can retard the corresponding diffusion process (i.e., simultaneous outward diffusion of Al and inward diffusion of O). However, the porous TiO₂ will rapidly grow if the temperature exceeds 850 °C, which will lead to crack formation within the dense and protective Al₂O₃ outer-scale [5,6] and subsequent failure of the coatings. In addition to the oxidation resistance, the

age hardening ability around 900 °C originated from the coherent strain between nano-scale c-TiN- and c-AlN-rich domains via spinodal decomposition makes c-TiAlN coatings attractive for advanced machining processes [1,2]. However, the metastable c-AlN-rich phase will transform into its stable structure hexagonal (h) AlN during further annealing treatments which can cause a rapid deterioration of mechanical properties [1]. Therefore, numerous attempts have been made to improve the performances of c-TiAlN to meet the requirements for severe industrial applications up to now. One of the successful methods is to add the alloying transition metals, such as Zr, Cr, Ta etc., to the c-TiAlN system to form quaternary nitride coatings [7-12].

For Zr-containing TiAlN coatings, the thermal stability is substantially improved [7,9], as experimentally observed via differential scanning calorimetry (DSC) by one of the present authors [7]. In Ref. 7, the transformation peak of c-AlN-rich-to-h-AlN locates at 1280 °C for Ti_{0.34}Al_{0.37}Zr_{0.29}N, which is higher than that of the Ti_{0.48}Al_{0.52}N by 70°C. Moreover, the addition of Zr in Ti_{1-x-y}Al_xZr_yN (x = 0.55, y = 0.05 and x = 0.51, y = 0.10) also promotes

Corresponding author: xueyun168@gmail.com* , lijun.zhang@csu.edu.cn[#]



the formation of TiN-, ZrN- and AlN-rich cubic domains as shown in the work of Chen et al. [7], indicating an earlier onset of spinodal decomposition compared with TiAlN coatings. For instance, as the amount of ZrN decreases from 0.10 to 0.05 to 0 (in mole fraction) the peak position of spinodal decomposition increases from 740 °C for $\text{Ti}_{0.39}\text{Al}_{0.51}\text{Zr}_{0.10}\text{N}$ to 760 °C for $\text{Ti}_{0.40}\text{Al}_{0.55}\text{Zr}_{0.05}\text{N}$, and to 800 °C for $\text{Ti}_{0.52}\text{Al}_{0.48}\text{N}$. In addition to the thermal stability, alloying Zr into TiAlN also significantly enhances the oxidation resistance as well as mechanical properties [7-9].

In order to further improve the performance of c-TiAlZrN coatings, quantitative description of microstructure evolution in metastable c-TiAlZrN coatings during service life is a prerequisite. Recent studies indicate that the underlying numerical simulations, like Cahn-Hilliard modeling [13] as well as phase-field method [14], are powerful and effective tools for microstructure evolution during spinodal decomposition. For further quantitative simulations, the coupling to CALPHAD (CALculation of PHase Diagram) thermodynamic databases [15,16], which can provide accurate thermodynamic information (like energy, potential, driving force, etc.) during the numerical simulation, is necessary [17-22]. Very recently, by combining the experimental equilibria on spinodal decomposition with first-principles computed free energies [23], a complete metastable phase diagram and the corresponding self-consistent thermodynamic description for the pseudo-binary c-TiN/c-AlN system were constructed in our previous work by means of CALPHAD method, based on which quantitative numerical simulations of spinodal decomposition were performed in both monolithic [23] and multilayer [24] c-TiAlN and c-TiAlN/TiN coatings. Though some first-principles calculations [10,25] and experimental investigations [7-10] on phase equilibria in metastable c-TiAlZrN system have been performed in the literature, no any attempt to establish a suitable CALPHAD thermodynamic database for metastable phase equilibria in c-TiAlZrN coatings is available.

Therefore, the major aim of the present work is to establish a reliable thermodynamic description for metastable c-TiAlZrN multicomponent system by means of the CALPHAD method with the aid of first-principles computed free energies as well as the experimental metastable phase equilibria.

2. Literature review

Prior to the evaluation of the experimental data, it is necessary to elaborate on the criteria for judging whether the c- $\text{Ti}_{1-x-y}\text{Al}_x\text{Zr}_y\text{N}$ coatings decompose spinodally at specified temperatures. In analogy to c- $\text{Ti}_{1-x}\text{Al}_x\text{N}$ coatings, the observation of c-(Ti,Al,Zr)N

(200) X-ray diffraction (XRD) peak broadening, asymmetry, shoulder peak formation, and the existence of c-AlN are the essentially characteristic features for spinodal decomposition [1,2]. According to the structural investigations via XRD, whether the c-(Ti,Al,Zr)N coatings annealed from low temperature toward high temperature decompose spinodally corresponds to the three cases in turn: *i*) that the broadening or asymmetry of (200) peak, the obvious shoulder formation of c-TiN, c-AlN or c-ZrN as well as the existence of all the features can be regarded as the occurrence of spinodal decomposition; *ii*) that the stage that incomplete transformation from metastable c-AlN to stable h-AlN with increasing temperature can also be regarded as spinodal decomposition; *iii*) that no c-AlN found but all h-AlN or other phases observed represents no spinodal decomposition at higher temperatures. Besides the XRD measurement, the typical features of spinodal decomposition obtained from other techniques were also combined to perform the evaluation, such as the observation of coherent phases with cubic structure from high resolution transmission electron microscopy (HRTEM), the modulation structure from scanning transmission electron microscopy (STEM) or atom probe tomography (APT), the endothermal peak responsible for spinodal decomposition from DSC, the age-hardening from nanoindentation measurements and so on. Base on the above criteria, all the experimental phase equilibrium information available in the literature is summarized in Table 1 and briefly described as follows.

The structure evolution of c-TiAlZrN was investigated by one of the present authors [7] using XRD on post deposition annealed coatings, and their results indicate that spinodal decompositions of c- $\text{Ti}_{1-x-y}\text{Al}_x\text{Zr}_y\text{N}$ coatings with $x = 0.55$, $y = 0.05$ and $x = 0.51$ and $y = 0.10$ take place from 700 ~ 1200 °C, forming c-TiN-, c-AlN- and c-ZrN-rich coherent domains. When the temperature reaches up to 1500 °C, there were no any signs of spinodal decomposition in either c- $\text{Ti}_{1-x-y}\text{Al}_x\text{Zr}_y\text{N}$ coatings according to Chen et al. [7]. For the c- $\text{Ti}_{0.34}\text{Al}_{0.37}\text{Zr}_{0.29}\text{N}$ coatings with slightly higher Zr contents, the spinodal decomposition occurs at 850 °C rather than 700 °C, and persists to 1300 °C [7]. Similarly, no spinodal decomposition is observed at 1500 °C.

Later, by means of the same approach, Abadias et al. [8] studied the thermal stability of high Zr- and low Al-containing quaternary $\text{Ti}_{1-x-y}\text{Al}_x\text{Zr}_y\text{N}$ coatings. Their experimental results after annealing at 600 °C showed that the investigated coatings with $x = 0.02$, $y = 0.48$ and $x = 0.04$, $y = 0.46$ are thermodynamically stable with main defect annihilation as well as crystal recovery, and phase decomposition takes place at 950 °C resulting in the formation of c-TiN-rich and c-ZrN-



rich domains. Lind et al. [10] observed that the spinodal decomposition occurs at 1100 and 1050 °C for the $c\text{-Ti}_{1-x-y}\text{Al}_x\text{Zr}_y\text{N}$ coatings with $x = 0.46$, $y = 0.24$ via ex-situ and in-situ XRD, and c-AlN-, c-TiN- and c-ZrN-rich domains form based on the STEM micrographs showing dark regions and brighter regions with obvious contrast. For the other higher Zr-containing $c\text{-Ti}_{1-x-y}\text{Al}_x\text{Zr}_y\text{N}$ coating with $x = 0.18$ and $y = 0.69$, no sign of spinodal decomposition exists in the XRD diffractogram at 1100 °C [10]. Instead, a binodal decomposition mechanism was proposed because much finer microstructure with dark and bright regions without contrast was observed in the STEM micrograph, compared with the former one under the same conditions. Very recently, based on their XRD measurements, Glatz et al. [9] reported that the $c\text{-Ti}_{1-x-y}\text{Al}_x\text{Zr}_y\text{N}$ coating with $x = 0.44$ and $y = 0.07$ undergoes spinodal decomposition from 900 ~ 1300 °C, and no sign of spinodal decomposition can be observed at 600, 700, 800 and 1400 °C. Meanwhile, the isostructure decomposition occurs in the $c\text{-Ti}_{1-x-y}\text{Al}_x\text{Zr}_y\text{N}$ coating with $x = 0.54$ and $y = 0.07$ at 1000 °C but not at 1400 °C [9].

isostructural c-TiN- and c-AlN-rich domains has been well acknowledged from both theoretical calculations [26,27] and experimental measurements [1,2]. Compared with c-TiAlN, c-ZrAlN possesses an even stronger tendency for the isostructural decomposition due to the very high and positive calculated formation energy [25, 28-30], and was also experimentally verified to decompose into c-ZrN- and c-AlN-rich domains and concomitant age-hardening [3,31]. It is noted that the total energy of c-TiZrN with respect to c-TiN and c-ZrN were shown to be positive for all the composition range via the first-principles calculations [4, 28, 32, 33], which can provide driving force for spinodal decomposition. Moreover, Abadias et al. [8] confirmed experimentally the phase separation of metastable c-TiZrN into c-TiN- and c-ZrN-rich phases at 950 °C via spinodal decomposition.

Since c-TiAlN, c-ZrAlN and c-TiZrN decompose spinodally into their respective two-phase cubic-structure counterparts, i.e., c-TiN/c-AlN, c-ZrN/c-AlN and c-TiN/c-ZrN, they are all regarded to be the constitutive pseudo-binary systems of the c-TiN/c-AlN/c-ZrN pseudo-ternary system. As for the

Table 1. Summary of the experimental equilibria (in mole fraction of Al and Zr) as well as the corresponding process parameters on spinodal decomposition of metastable $c\text{-Ti}_{1-x-y}\text{Al}_x\text{Zr}_y\text{N}$ coatings

x	y	With spinodal decomposition (°C)	Without spinodal decomposition (°C)	Deposition parameters			Annealing parameters		Refs.
				Method	Bias (V)	Pressure (Pa)	Method	Time (h)	
0.55	0.05	700, 850, 1100, 1200	1500	RUMS	-60	<0.8mPa	DSC		[7]
0.51	0.10	700, 850, 1100, 1200	1500						
0.37	0.29	850, 950, 1100, 1200, 1300	700, 1500						
0.02	0.48	950	600	RUMS		0.2	VF	2	[8]
0.04	0.46	950	600						
0.46	0.24	1050, 1100		RCAE	-30	3.5	In-situ XRD		[10]
0.18	0.69		1100				VF	2	
0.44	0.07	900, 1000, 1100, 1200, 1300	600, 700, 800, 1400	RCAE	-80	3.5	VF		[9]
0.54	0.07	1000	1400						

RCAE = Reactive cathodic arc evaporation, RUMS = Reactive unbalance magnetron sputtering, VF = Vacuum furnace

3. Thermodynamic model

Before performing the CALPHAD assessment, the physically-sound thermodynamic model for c-TiAlZrN system should be determined a priori. The spinodal decomposition of metastable c-TiAlN into

quaternary c-TiAlZrN, Chen et al. [7] demonstrated the formation of c-TiN-, c-AlN- and c-ZrN-rich domains after spinodal decomposition via the post deposition annealed coatings, which was confirmed in the later reports from the other research groups [9, 10]. Moreover, Lind et al. [10] predicted that the final



result of spinodal decomposition should be c-TiN, c-AlN and c-TiZrN via the first-principles calculations. They also suggested that the phase separation between c-AlN and c-ZrN occurs first due to the very high and positive formation energy even at 1300 K compared with c-TiAlN.

Consequently, the single c-TiAlZrN phase is regarded to be a pseudo-ternary system consisting of three species, i.e., c-TiN, c-AlN and c-ZrN, and is thus modeled as a disordered substitutional solution phase. Its Gibbs energy can be described using the Redlich-Kister (R-K) polynomial [34]:

$$G_{c-TiAlZrN}^m - H^{\text{SER}} = {}^0G_{c-TiN} \cdot x_{c-TiN} + {}^0G_{c-AlN} \cdot x_{c-AlN} + {}^0G_{c-ZrN} \cdot x_{c-ZrN} \\ + RT \cdot (x_{c-TiN} \cdot \ln x_{c-TiN} + x_{c-AlN} \cdot \ln x_{c-AlN} + x_{c-ZrN} \cdot \ln x_{c-ZrN}) \\ + x_{c-TiN} \cdot x_{c-AlN} \cdot L_{c-TiN,c-AlN} + x_{c-TiN} \cdot x_{c-ZrN} \cdot L_{c-TiN,c-ZrN} \\ + x_{c-AlN} \cdot x_{c-ZrN} \cdot L_{c-AlN,c-ZrN} + {}^{\text{ex}}G_{c-TiN,c-AlN,c-ZrN} \quad (1)$$

with the excess Gibbs energy ${}^{\text{ex}}G_{c-TiN,c-AlN,c-ZrN}$ expressed as

$${}^{\text{ex}}G_{c-TiN,c-AlN,c-ZrN} = x_{c-TiN} \cdot x_{c-AlN} \cdot x_{c-ZrN} \\ \cdot (x_{c-TiN} \cdot L_{c-TiN} + x_{c-AlN} \cdot L_{c-AlN} + x_{c-ZrN} \cdot L_{c-ZrN}) \quad (2)$$

In Eq. (1), R is the gas constant, T is the absolute temperature, while x_{c-TiN} , x_{c-AlN} and x_{c-ZrN} are the mole fractions of species c-TiN, c-AlN and c-ZrN, respectively. ${}^0G_{c-TiN}$, ${}^0G_{c-AlN}$ and ${}^0G_{c-ZrN}$ are Gibbs energy for the species c-TiN, c-AlN and c-ZrN, of which the reference states are used by the stable element reference (SER), i.e. the molar enthalpy of component i (i.e., c-TiN, c-AlN or c-ZrN) at 298.15 K and 1 bar. The Gibbs energies of species c-TiN, c-AlN and c-ZrN are directly taken from the first-principles calculations by Wang et al. [35]. $L_{i,j}$ s and L_i s ($i, j = \text{c-TiN, c-AlN, or c-ZrN}$) are the binary and ternary interaction parameters in respective boundary binary and ternary systems, which are expressed as:

$$L_{i(j)} = a + b \cdot T \quad (3)$$

The parameters a and b are to be assessed on the basis of the experimental phase equilibria and first-principles computed thermodynamic properties.

4. Results and discussion

Evaluation of the thermodynamic parameters was attained by recurrent runs of PARROT program [36] in order to achieve best fit to the experimental data. The thermodynamic optimization begins with the three boundary pseudo-binary c-TiN/c-AlN, c-AlN/c-ZrN, c-TiN/c-ZrN systems. $L_{TiN,AlN}$ s in c-TiN/c-AlN quasi-binary system were directly taken from our previous work [23], in which four interaction parameters are enough to reproduce most of the experimental data. As for the other two systems, no

thermodynamic assessments are available in the literature due to the lack of experimental information. Thus, in the present work, the thermodynamic descriptions in the c-TiN/c-ZrN and c-AlN/c-ZrN pseudo-binary systems were evaluated based on the first-principles computed thermochemical data in combination with the experimental phase equilibrium data in the pseudo-ternary system. Specifically, $L_{TiN,ZrN}$ s in the c-TiN/c-ZrN system were obtained by directly reproducing the calculated temperature-composition diagram [28] considering the vibration effect at 0 GPa. Due to some discrepancies between the experimental and theoretical investigations, $L_{AlN,ZrN}$ s in c-AlN/c-ZrN based on the first-principles calculations [28] were re-adjusted to achieve a good fit to the experimental data. Afterwards, the thermodynamic descriptions for the three pseudo-binary c-TiN/c-AlN, c-AlN/c-ZrN, c-TiN/c-ZrN systems can be evaluated. The ternary interaction parameters were then assessed according to the experimental data critically reviewed in Section 2, following the similar the finally strategy demonstrated in our previous work [23]. Thus obtained thermodynamic descriptions for the c-TiN/c-AlN/c-ZrN pseudo ternary system in the present work are listed in Table 2.

The calculated metastable phase equilibria for the three pseudo-binary systems are displayed in Fig. 1 (a), (b) and (c), respectively, according to the thermodynamic descriptions evaluated by Zhou et al. [23] (c-TiN/c-AlN), the first-principles calculation [28] (c-TiN/c-ZrN) and in the present work (c-AlN/c-ZrN). The solid lines denote the computed binodal curves while the dotted lines represent the calculated spinodal curves. The obtained critical point of the metastable c-TiN/c-AlN miscibility gap lies at 1837 °C with $x_{AlN} = 0.39$ (Fig. 1 a), while that of the metastable c-TiN/c-ZrN system at 1606 °C with $x_{ZrN} = 0.35$ (Fig. 1 b). Moreover, the recent first-principles calculated c-AlN/c-ZrN miscibility gaps resulted in extremely high temperatures for the critical point up to 12500 K [28] and 25000 K [29], respectively, due to the usage of a constant value of the interaction parameter calculated at 0 K. However, the c-AlN/c-ZrN miscibility gap re-adjusted based on the first-principles calculations and experimental data has the

Table 2 Summary of the thermodynamic parameters in the pseudo-ternary c-TiN/c-AlN/c-ZrN system obtained in the present work

fcc: Model (TiN, AlN, ZrN) ₁	Refs.
$L_{c-TiN,c-AlN} = 22129.97 + 5.25T + (-15.24 + 2.64T)(x_{c-TiN} - x_{c-AlN})$	[23]
$L_{c-TiN,c-ZrN} = 42294.19 - 7.76T + (6024.33 + 0.72T)(x_{c-TiN} - x_{c-ZrN})$	[28]
$L_{c-AlN,c-ZrN} = 201137.88 - 91.53T + (143088.23 - 73.05T)(x_{c-AlN} - x_{c-ZrN})$	This work
${}^{\text{ex}}G_{c-TiN,c-AlN,c-ZrN} = x_{c-TiN} \cdot x_{c-AlN} \cdot x_{c-ZrN} \cdot [(9702.50 + 7.50T)x_{c-TiN} \\ + (67208.25 - 5.25T)x_{c-AlN} + (-18421.00 - 23.00T)x_{c-ZrN}]$	This work



consolute temperature at 1607 °C with $x_{ZrN} = 0.38$, as presented in Fig. 1 c. Based on the three metastable c-TiN/c-AlN, c-AlN/c-ZrN and c-TiN/c-ZrN phase diagrams together with the assessed ternary interaction parameters, the metastable ternary c-TiN/c-AlN/c-ZrN can be constituted, as shown in Fig. 2 for visualization.

The calculated isothermal sections of the pseudo-

ternary c-TiN/c-AlN/c-ZrN system at 850 ~ 1500 °C according to the present thermodynamic descriptions are presented in Figs. 3 and 4, together with the experimental data critically reviewed in Section 2. In the figures, the solid lines denote the calculated metastable phase boundaries, the dotted lines the spinodal curves for two decomposed phases, while the dot-dashed lines the spinodal curves for three

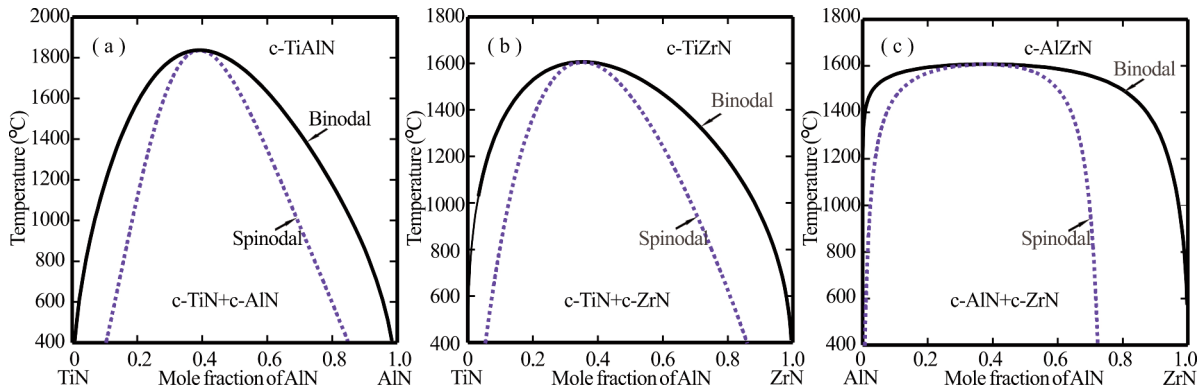


Figure 1. Calculated metastable phase equilibria in (a) c-TiN/c-AlN [23], (b) c-TiN/c-ZrN [28], and (c) c-AlN/c-ZrN (this work) pseudo binary systems with the solid and dotted lines denoting the binodal and spinodal curves, respectively

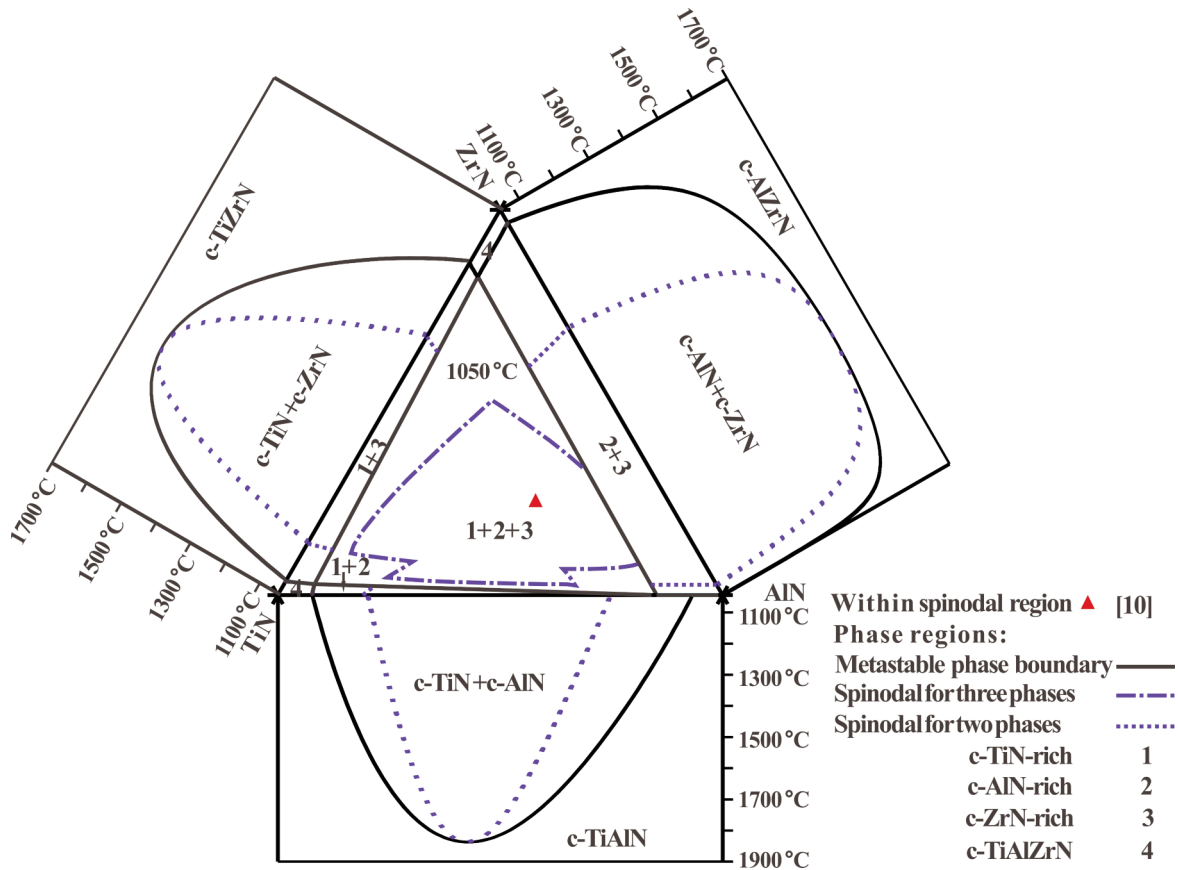


Figure 2. Metastable ternary c-TiN/c-AlN/c-ZrN phase diagram constituted by metastable binary c-TiN/c-AlN, c-AlN/c-ZrN and c-TiN/c-ZrN phase diagrams combining the three interaction parameters



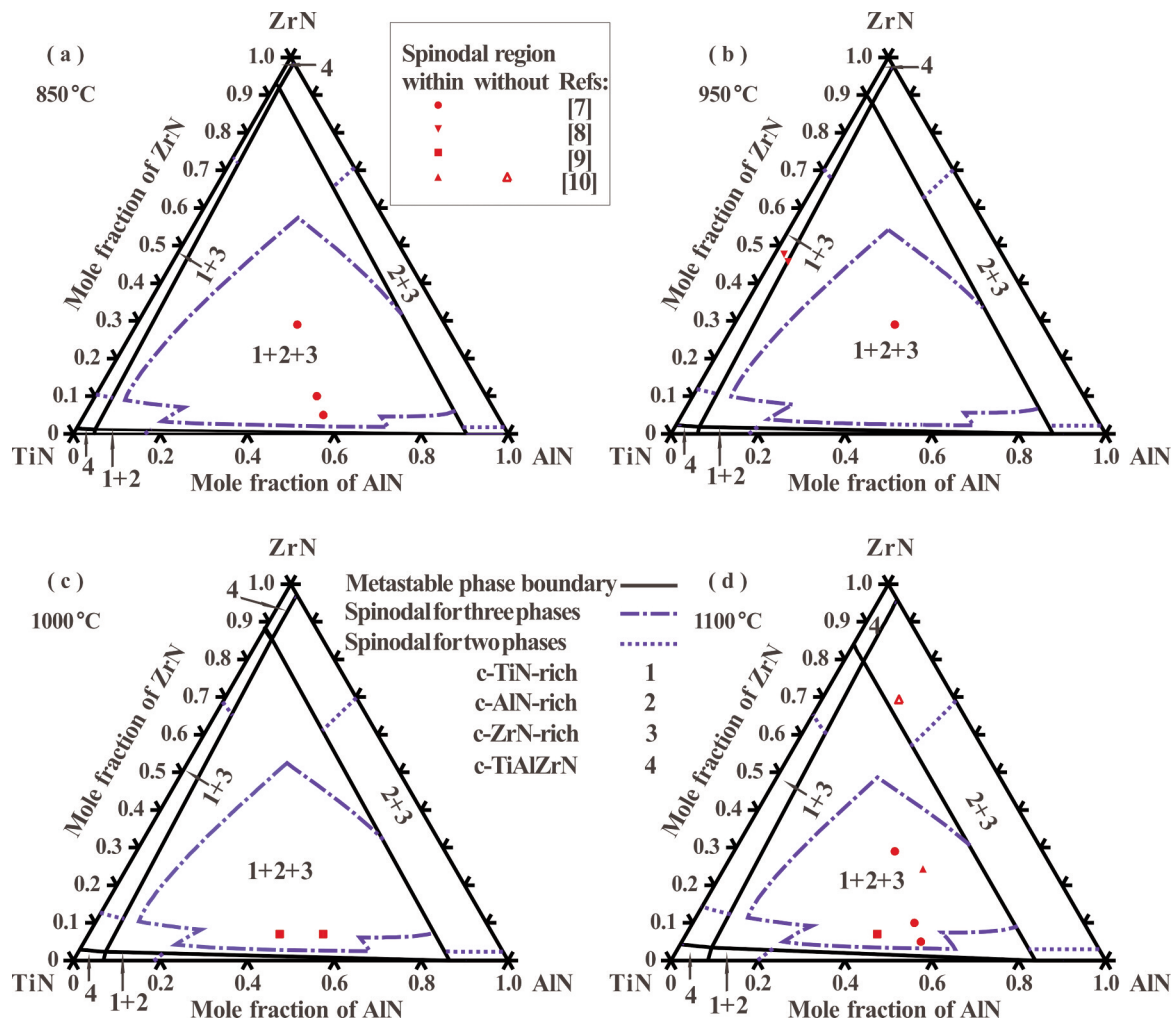


Figure 3. Calculated isothermal sections of pseudo-ternary $c\text{-TiN}/c\text{-AlN}/c\text{-ZrN}$ system at 850, 950, 1000, and 1100 °C according to the present thermodynamic description, compared with the experimental data [7-10]. The solid lines are the calculated binodal curves, the dotted lines the spinodal curves for two decomposed phases, while the dot-dashed lines the spinodal curves for three decomposed phases

decomposed phases. The solid and hollow patterns represent the experimental data with and without spinodal decomposition evaluated in Section 2, which should locate inside and outside the spinodal regions, respectively. As can be seen, the experimental data occurring spinodal decomposition at 850, 950, 1100, 1200 and 1300 °C from the work of Chen et al. [7] just locates in spinodal regions for three decomposed phases, which is consistent with the experimental results that the metastable $c\text{-TiAlZrN}$ decomposes spinodally into $c\text{-TiN}$ -, $c\text{-AlN}$ - and $c\text{-ZrN}$ -rich domains [7], while no spinodal decomposition happens when the coating is annealed at 1500 °C except for a small deviation of the $c\text{-Ti}_{1-x-y}\text{Al}_x\text{Zr}_y\text{N}$ coating with $x = 0.37$ and $y = 0.29$.

For the case that a small amount of Al in $c\text{-TiZrN}$, the $c\text{-Ti}_{1-x-y}\text{Al}_x\text{Zr}_y\text{N}$ coatings with $x = 0.02$, $y = 0.48$ and $x = 0.04$, $y = 0.46$ at 950 °C (Fig. 3b) lie in the

two-phase spinodal decomposition domain near the $c\text{-TiN}/c\text{-ZrN}$ side, which have been experimentally verified to segregate into $c\text{-TiN}$ - and $c\text{-ZrN}$ -rich phases by Abadias et al. [8]. For the high Zr-containing $c\text{-Ti}_{1-x-y}\text{Al}_x\text{Zr}_y\text{N}$ coatings with more than 75 ~ 80 % ZrN, Lind et al. [10] theoretically predicted that the decomposition mechanism is unlikely the spinodal one, and experimentally confirmed that the decomposition of $c\text{-Ti}_{1-x-y}\text{Al}_x\text{Zr}_y\text{N}$ coating with $x = 0.18$ and $y = 0.69$ at 1100 °C (Fig. 3d) conduct through the binodal one. The binodal decomposition is via nucleation and growth mechanism resulting in a much finer (approximately 5 times small) microstructure for $\text{Ti}_{0.13}\text{Al}_{0.18}\text{Zr}_{0.69}\text{N}$ after annealing 2 h compared with that for $\text{Ti}_{0.30}\text{Al}_{0.24}\text{Zr}_{0.46}\text{N}$ [10] which is highly unstable against spinodal decomposition at 1050 and 1100 °C (Fig. 3d). Moreover, the $c\text{-Ti}_{1-x-y}\text{Al}_x\text{Zr}_y\text{N}$ coatings with low ZrN content $x = 0.44$, $y =$

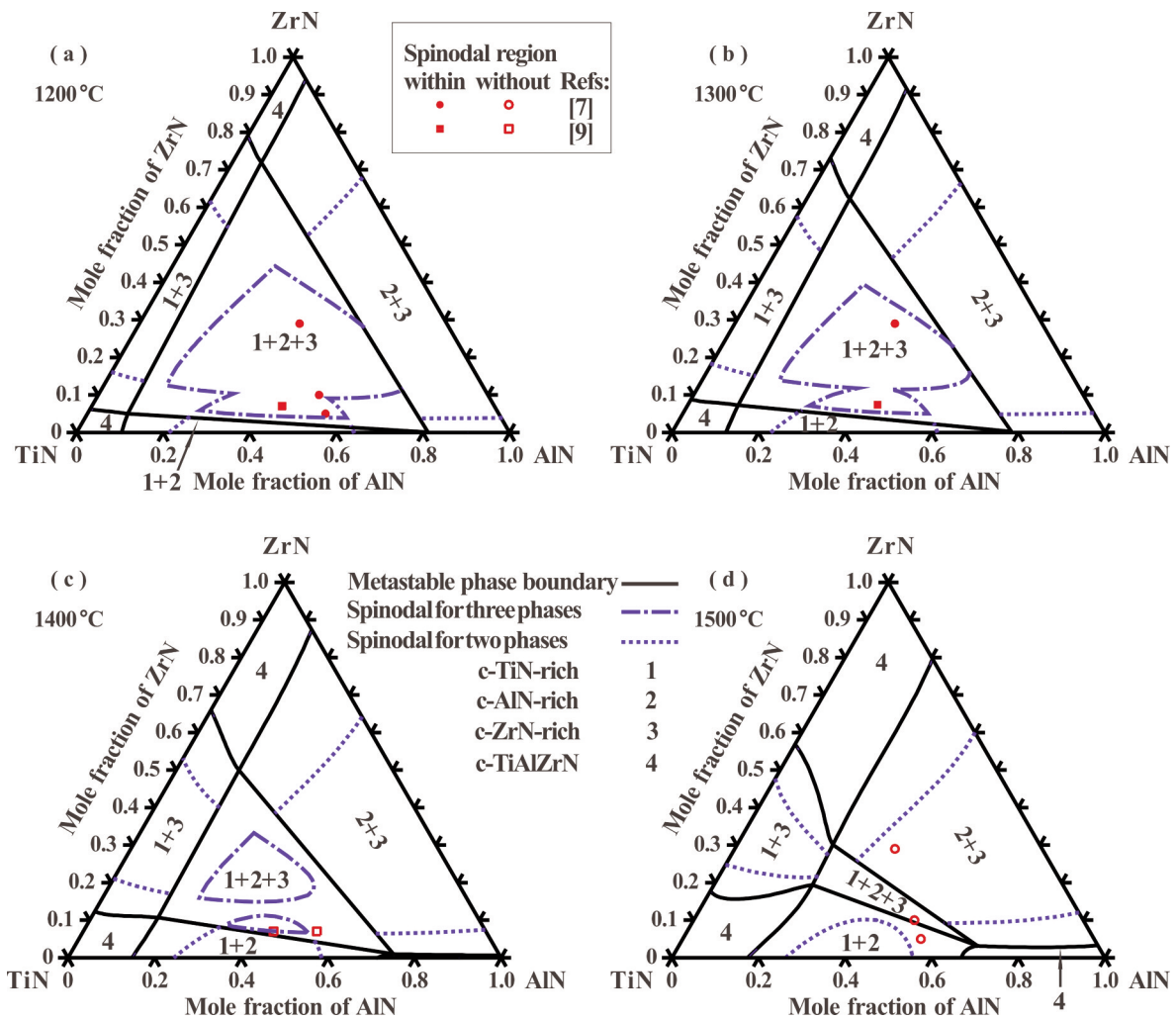


Figure 4. Calculated isothermal sections of pseudo-ternary c-TiN/c-AlN/c-ZrN system at 1200, 1300, 1400, and 1500 °C according to the presently evaluated thermodynamic description, compared with the experimental data [7, 9]. The solid lines are the calculated binodal curves, the dotted lines the spinodal curves for two decomposed phases, while the dot-dashed lines the spinodal curves for three decomposed phases

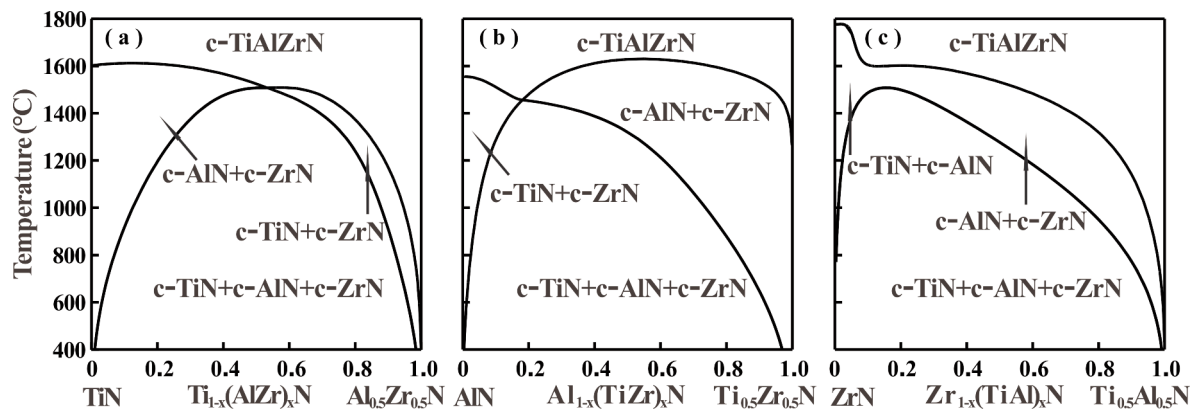


Figure 5. Model-predicted vertical sections along (a) TiN- $Al_{0.5}Zr_{0.5}N$, (b) AlN- $Ti_{0.5}Zr_{0.5}N$ and (c) ZrN- $Ti_{0.5}Al_{0.5}N$ in the pseudo-ternary c-TiN/c-AlN/c-ZrN system according to the present thermodynamic description



0.07 at 1000, 1100, 1200 1300 °C and $x = 0.54$, $y = 0.07$ at 1000 °C also locate in the spinodal domain in the pseudo-ternary system, but not at 1400 °C which are consistent with the experimental results [9]. The good agreement between the calculated phase equilibria and the experimental data over the wide temperature range validate the reliability of the present thermodynamic descriptions for the c-TiAlZrN system.

Based on the present thermodynamic descriptions for the c-TiAlZrN system, different phase diagrams and thermodynamic properties can be predicted. For instance in Fig. 5, three vertical sections along TiN- $\text{Al}_{0.5}\text{Zr}_{0.5}\text{N}$, AlN- $\text{Ti}_{0.5}\text{Zr}_{0.5}\text{N}$ and ZrN- $\text{Ti}_{0.5}\text{Al}_{0.5}\text{N}$ are calculated on the basis of the present thermodynamic descriptions. From such plots, one can easily see the evolution of phase regions at different compositions along temperature. Moreover, the model-predicted standard enthalpies of formation in the pseudo-ternary c-TiN/c-AlN/c-ZrN system over the entire composition range are displayed in Fig. 6. As can be seen, the slight positive enthalpies of formation indicate that the pseudo-ternary system is metastable with respect to the cubic binary nitrides. In addition, the driving force for decomposition is slightly larger close to the AlN-rich region.

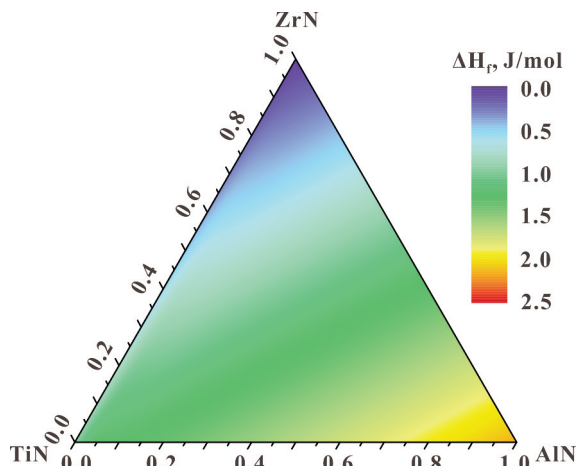


Figure 6. Model-predicted standard enthalpies of formation in the pseudo-ternary c-TiN/c-AlN/c-ZrN system over the entire composition range

5. Summary

Based on the experimental observations of the triple spinodally decomposed domains, the metastable c-TiAlZrN coatings were treated as a pseudo-ternary c-TiN/c-AlN/c-ZrN system, and described as a substitutional solution phase. A CALPHAD thermodynamic assessment of the pseudo-ternary c-TiN/c-AlN/c-ZrN system was then conducted on the basis of the limited experimental data and the first-

principles computed free energies. The theoretically-predicted thermodynamic description of the metastable pseudo-binary c-AlN/c-ZrN system, which deviates from experimental results, was re-adjusted to fit the experimental information in the pseudo-ternary c-TiN/c-AlN/c-ZrN system. Most of the experimental data in the metastable c-TiAlZrN coatings over the wide temperature range were reproduced well, indicating that the presently obtained thermodynamic descriptions for the metastable c-TiAlZrN coatings are reliable. With the present thermodynamic description, a variety of phase diagrams and thermodynamic properties in the metastable c-TiAlZrN coatings can be nicely predicted. Furthermore, the present thermodynamic descriptions can provide accurate thermodynamic information for further quantitative numerical description of microstructure evolution in TiAlZrN-based coatings.

Acknowledgement

The financial support from the National Natural Science Foundation of China (Grant Nos. 51474239 and 51371201) and the National Science and Technology Major Project of China (Grant No. 2015ZX04005008) is greatly acknowledged. Jingjing Zhou acknowledges support from Lanzhou Institute of Technology (Grant No. 2014K-013).

References

- [1] P.H. Mayrhofer, A. Hörling, L. Karlsson, J. Sjölen, T. Larsson, C. Mitterer, L. Hultman, *Appl. Phys. Lett.* 83 (2003) 2049-2051.
- [2] A. Hörling, L. Hultman, M. Odén, J. Sjölen, L. Karlsson, *J. Vac. Sci. Technol. A* 20 (2002) 1815-1823.
- [3] L. Rogström, L.J.S. Johnson, M.P. Johansson, M. Ahlgren, L. Hultman, M. Odén, *Scripta Mater.* 62 (2010) 793-741.
- [4] A. Hoerling, J. Sjölen, H. Willmann, T. Larsson, M. Odén, L. Hultman, *Thin Solid Films* 516 (2008) 6421-6431.
- [5] F. Vaz, L. Rebouta, M. Andritschky, M.F.d. Silva, J.C. Soares, *J. Eur. Ceram. Soc.* 97 (1997) 1971-1977.
- [6] D. McIntyre, J.E. Greene, G. Hakansson, J.E. Sundgren, W.D. Münz, *J. Appl. Phys.* 67 (1990) 1542-1553.
- [7] L. Chen, D. Holec, Y. Du, P.H. Mayrhofer, *Thin Solid Films* 519 (2011) 5503-5510.
- [8] G. Abadias, I.A. Saladukhin, V.V. Uglov, S.V. Zlotski, D. Eyidi, *Surf. Coat. Technol.* 237 (2013) 187-195.
- [9] S.A. Glatz, R. Hollerweger, P. Polcik, R. Rachbauer, J. Paulitsch, P.H. Mayrhofer, *Surf. Coat. Technol.* 266 (2015) 1-9.
- [10] H. Lind, R. Pilemalm, L. Rogström, F. Tasnadi, N. Ghafoor, R. Forsén, L.J. S. Johnson, M.P. Johansson-Jöesaar, M. Odén, I.A. Abrikosov, *AIP Adv.* 4 (2014) 127147.
- [11] Y.X. Xu, L. Chen, B. Yang, Y.B. Peng, Y. Du, J.C. Feng, F. Pei, *Surf. Coat. Technol.* 235 (2013) 506-512.



- [12] R. Rachbauer, D. Holec, P.H. Mayrhofer, Surf. Coat. Technol. 211 (2012) 98-103.
- [13] J.W. Cahn, J.E. Hilliard, J. Chem. Phys. 28 (1958) 258-267.
- [14] I. Steinbach, Annu. Rev. of Mater. Res. 43 (2013) 89-107.
- [15] www.thermocalc.com/products-services/databases/thermodynamic/.
- [16] L. Zhang, J. Wang, Y. Du, R. Hu, P. Nash, X.-G. Lu, C. Jiang, Acta Mater. 57 (2009) 5324-5341.
- [17] J.Z. Zhu, Z.K. Liu, V. Vaithyanathan, L.Q. Chen, Scripta Mater. 46 (2002) 401-406.
- [18] I. Steinbach, B. Böttger, J. Eiken, N. Warnken, S.G. Fries, J. Phase Equilib. Diff. 28 (2007) 101-106.
- [19] L. Zhang, Y. Du, J. Phase Equilib. Diff. 37 (2016) 259-260.
- [20] L. Zhang, M. Stratmann, Y. Du, B. Sundman, I. Steinbach, Acta Mater. 88 (2015) 156-169.
- [21] M. Wei, Y. Tang, L. Zhang, W. Sun, Y. Du, Metall. Mater. Trans. A 46 (2015) 3182-3191.
- [22] X. Yang, Y. Tang, D. Cai, L. Zhang, Y. Du, S. Zhou, J. Min. Metall. Sect. B - Metall. 52 (2016) 77-85.
- [23] J. Zhou, J. Zhong, L. Chen, L. Zhang, Y. Du, Z.-K. Liu, P.H. Mayrhofer, CALPHAD 56 (2017) 92-101.
- [24] J. Zhou, L. Zhang, L. Chen, H. Wu, Y. Du, J. Micromech. Mol. Phys. 01 (2016) 1650002.
- [25] D. Holec, L. Zhou, R. Rachbauer, P.H. Mayrhofer, J. Appl. Phys. 113 (2013) 113510.
- [26] B. Alling, A.V. Ruban, A. Karimi, L. Hultman, I.A. Abrikosov, Phys. Rev. B 83 (2011) 104203.
- [27] P.H. Mayrhofer, D. Music, J.M. Schneider, Appl. Phys. Lett. 88 (2006) 071922.
- [28] A. Wang, S.-L. Shang, Y. Du, L. Chen, J. Wang, Z.-K. Liu, J. Mater. Sci. 47 (2012) 7621-7627.
- [29] S.H. Sheng, R.F. Zhang, S. Veprek, Acta Mater. 56 (2008) 968-976.
- [30] D. Holec, R. Rachbauer, L. Chen, L. Wang, D. Luef, P.H. Mayrhofer, Surf Coat Technol 206 (2011) 1698-1704.
- [31] R. Sanjinés, C.S. Sandu, R. Lamni, F. Lévy, Surf. Coat. Technol. 200 (2006) 6308-6312.
- [32] V. Petrman, J. Houska, J. Mater. Sci. 48 (2013) 7642-7651.
- [33] P. Ou, J. Wang, S. Shang, L. Chen, Y. Du, Z.-K. Liu, F. Zheng, Surf. Coat. Technol. 264 (2015) 41-48.
- [34] O. Redlich, A.T. Kister, Ind. Eng. Chem. 40 (1948) 345-348.
- [35] A. Wang, S. Shang, D. Zhao, J. Wang, L. Chen, Y. Du, Z.-K. Liu, T. Xu, S. Wang, Calphad 37 (2012) 126-131.
- [36] B. Sundman, B. Jansson, J.-O. Andersson, Calphad 9 (1985) 153-190.



